19. Y. J. Chabal, G. S. Higashi, K. Raghavachari, and V. A. Burros, *J. Vac. Sci. Technol. A*, **7**, 2104 (1989).
20. A. Venkateswara Rao, F. Ozanam, and J. N. Chazalviel, *This Journal*, **138**, 153 (1991).
21. C. M. Chong, S. R. Wenham, and M. A. Green, *Appl. Phys. Lett.*, **55**, 2363 (1989).

Electrochemical Control of Polyaniline Morphology as Studied by Scanning Tunneling Microscopy

Yeon-Taik Kim, Hongjun Yang, and Allen J. Bard*

Department of Chemistry and Biochemistry, The University of Texas at Austin, Austin, Texas 78712

ABSTRACT

The relation between structure and preparation conditions of polyaniline (PANI) was determined using scanning tunneling microscopy in air. The morphology of a PANI film grown with fast cyclic potential scans (20 V/s) was uniform and dense, whereas a film grown with slow scans (50 mV/s) over the same potential range with the same number of coulombs passed was amorphous and rough. The possibility of control of PANI morphology based on the electropolymerization kinetics is discussed.

Electrochemical control of the morphology during the early stages of polyaniline (PANI) growth is demonstrated by variation of the deposition rate. The structures of thin (<500 Å) electrochemically-formed PANI films were determined with a scanning tunneling microscope (STM) (1-5). The STM images were compared to those obtained with a scanning electron microscope (SEM). A uniform PANI structure was found when the film was electrodeposited with rapid cycling (20 V/s), but with slow scans (50 mV/s) a rougher, amorphous film was formed.

Conducting polymers (6-10), such as polypyrrole, PANI, and polythiophene, have been investigated in an attempt to understand the effect of preparation conditions on polymer structure. The electrochemical deposition conditions, *e.g.*, supporting electrolyte, solvent, and substrate, are important factors in determining the physical and chemical properties of the conducting films. Scanning electron microscopy (SEM) has been used to investigate the morphology of conducting polymers (6-10), but has not been of use in obtaining structural information about films less than a few hundred angstroms thick. Recently, the morphology of conducting polymers was investigated using an STM operated in air at a resolution of nm to μm (11-15). In this letter, STM images of PANI deposited by cyclic potential sweeps provide insight into the structure-preparation relationship of films.

An understanding of the electrochemistry and corresponding mechanism of film formation of PANI is difficult because of the complicated reaction kinetics involved in the electro-oxidation of aniline, particularly during the early stages of electrochemical deposition (16). To determine the effect of potential scan rate on film morphology, Pt film working electrodes were prepared by sputtering Pt on a glass slide. An STM image (500 nm × 500 nm) of this Pt film, see Fig. 1, showed a polycrystalline structure, with crystals in the size range 10-50 nm.

A cyclic voltammogram recorded at 50 mV/s at a Pt film electrode in a solution containing 20 mM aniline in 1*M* H_2SO_4 is shown in Fig. 2a. Following initial oxidation of aniline at about +0.5 V *vs.* SMSE, at least five different reduction and oxidation steps are observed, as is typical of aniline electropolymerization under these conditions (16, 17). The major growth mechanism of PANI has been described as occurring via the formation of dimeric species from the nucleophilic attack of the aniline on the nitrene cation radical, resulting in three different dimerization products (*i.e.*, head-to-head, head-to-tail, and tail-to-tail), as well as competitive degradation reactions (16).

PANI was deposited by passing a total anodic charge of approximately 35 mC/cm² (18). This yielded a film 450 ± 50 Å thick, as determined by electrochemical and spectroscopic ellipsometry measurements (19, 20). The typical surface morphology of a 5 × 5 μm area of the resulting PANI is shown in the STM image, Fig. 2b. Unlike the fiber structures determined by SEM with micrometer thick films of PANI (9), most of the surface structures appeared rather amorphous and did not show good resolution. The SEM images obtained for the PANI, prepared using the same conditions as in Fig. 2b, were typically similar to the STM image in Fig. 2b; the thicker aggregates seen in Fig. 2d were rarely observed. *In situ* electrochemical STM of PANI also produced images similar to Fig. 2b (21). When the STM scanning area was decreased to 100 by 100 nm, small lumps could occasionally be seen, Fig. 2c. The diameters of lumps varied over a range of 20-80 nm. Figure 2b shows a large amount of either a void fraction or surface roughness. When the roughness was estimated by height measurement (*e.g.*, peak to valley), the range of roughness was 200-400 Å for a number of different spots and samples. Sometimes under higher resolution the bare Pt surface, as in Fig. 1, could be resolved. The difference between the thicknesses estimated from the electrochemical methods and STM measurements is probably caused by an underestimation of the electrode area and uncertainties in thickness measurements with the STM.

When the electropolymerization was performed with a scan rate of 20 V/s, the resulting cyclic voltammogram, Fig. 3a, and film morphology, Fig. 3b, were very different. Only one set of large peaks (B, B′) is observed during the early stages of film growth. Smaller peaks (*e.g.*, A, A′) grow in during later scans. The oxidation peak (B) at 0.10 V *vs.* SMSE and the reduction peak (B′) at −0.10 V are at the same potentials as that shown by the head-to-tail dimer, 4-amino-diphenylamine (22). In the first scan, the ΔE_p for the B, B′ couple is approximately 200 mV; this increases with continuous scanning, probably because of increased uncompensated *iR* drop as the PANI grows

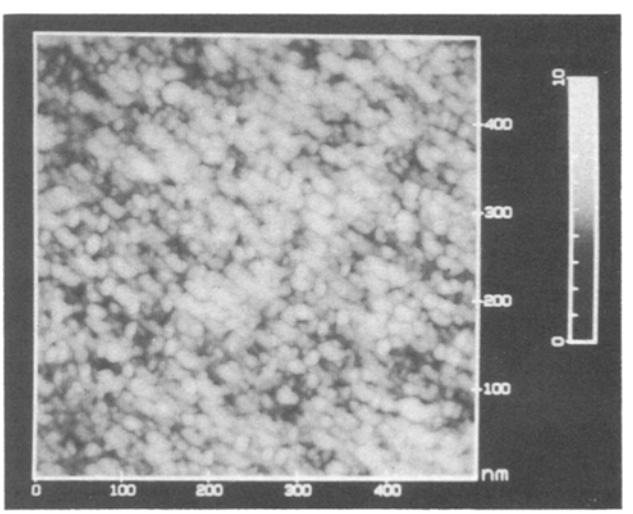

Fig. 1. STM image of the sputtered Pt film surface. V_b = 200 mV, i_t = 2.0 nA. The scanned area is 500 nm × 500 nm.

* Electrochemical Society Active Member.

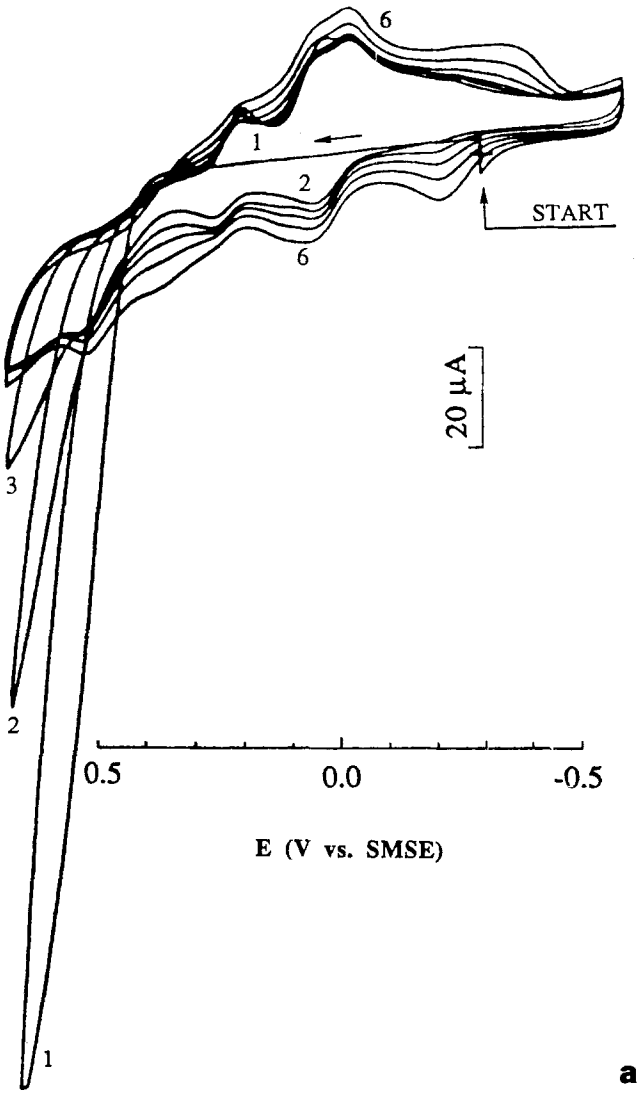

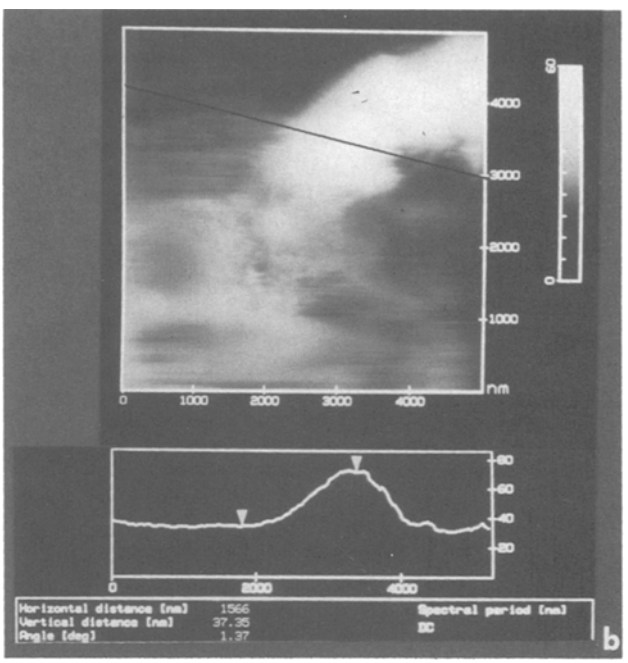

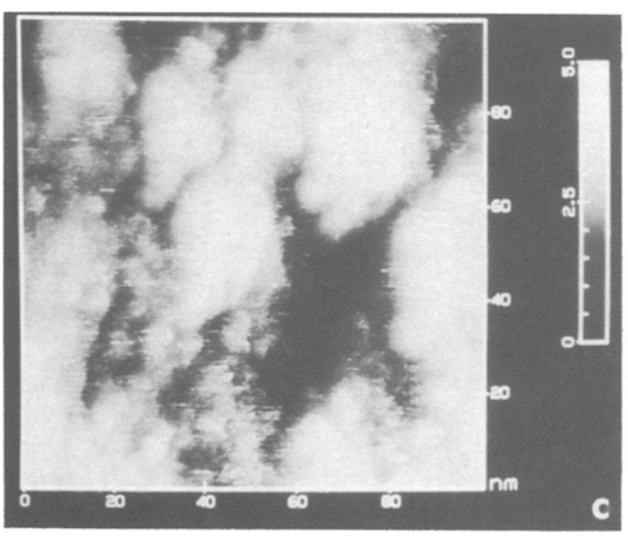

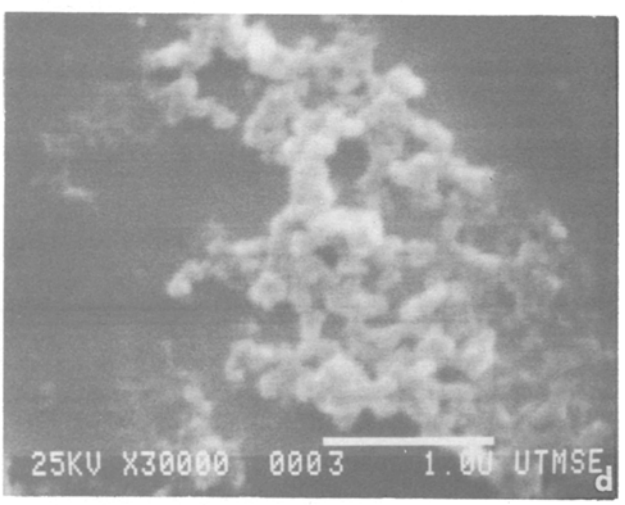

Fig. 2. (a) Cyclic voltammogram of PANI growth on Pt film at 50 mV/s, scanned between −0.6 and 0.7 V *vs.* a saturated mercurous sulfate electrode (SMSE). Solution, aqueous 1*M* H_2SO_4, 20 mM aniline. Electrode diameter, 2 mm. Numbers indicate scan number. (b) STM image in air of the PANI grown in Fig. 2a. V_b = −200 mV, i_t = 2.0 nA. The scanned area is 5 μm × 5 μm. Depth profile along the line is shown at the bottom. (c) STM image in air of the PANI grown in Fig. 2a. V_b = −200 mV, i_t = 2.0 nA. The scanned area is 100 nm × 100 nm. (d) SEM of the PANI grown in Fig. 2a.

thicker. After extensive cycling at this scan rate (~30 cycles), a cyclic voltammogram similar to Fig. 2a was found. The STM image of PANI deposited at 20 V/s after passage of 35 mC/cm^2 total anodic charge is shown in Fig. 3b. In this case, the film appears as particles of uniform size (*ca.* 10 × 60 × 350 nm) apparently composed of fiber bundles. PANI grows by nucleation, rather than layer-by-layer; the voids created as the fiber bundles form are filled by continuous bundle growth. When currents of more than 40 mC/cm^2 were passed, a complete coalescence was observed.

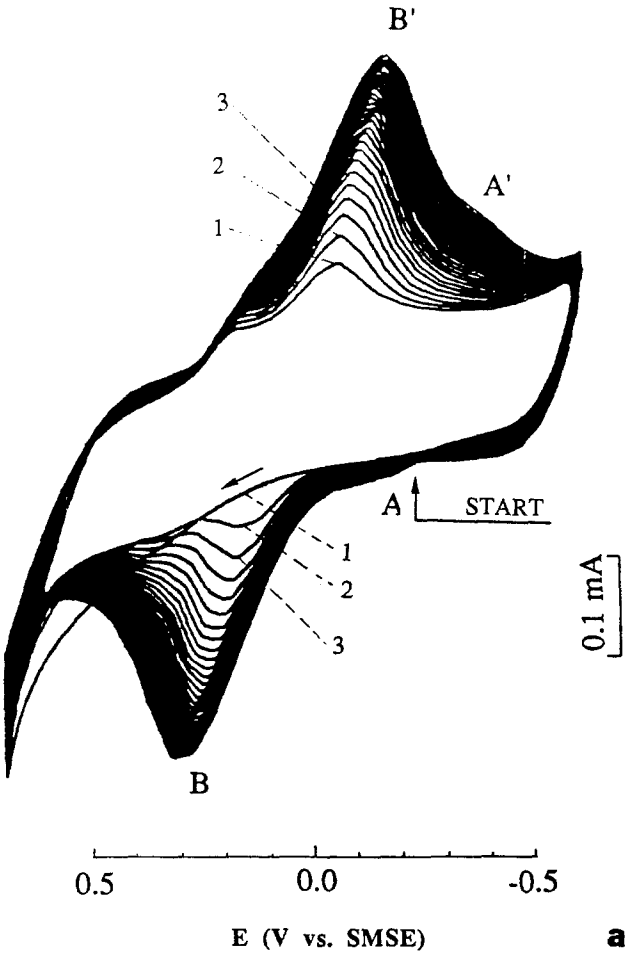

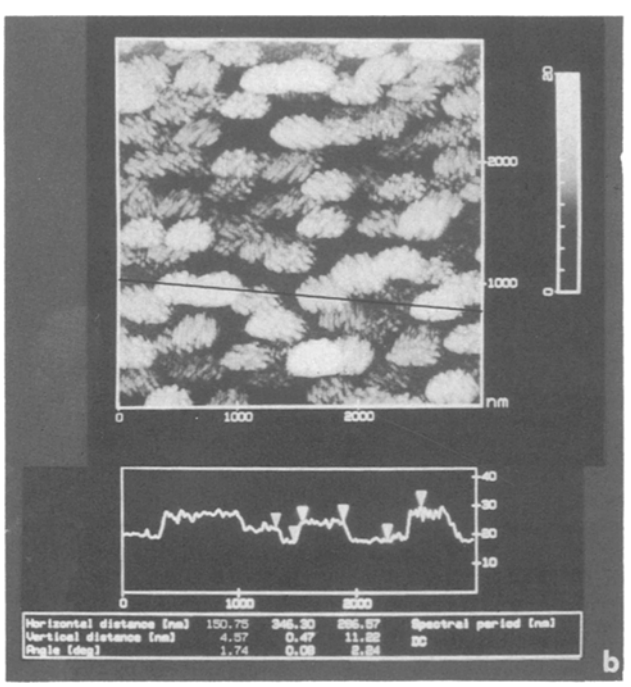

Fig. 3. (a) Cyclic voltammogram of PANI growth at 20 V/s, scanned between −0.6 and 0.7 V *vs.* SMSE. Solution, aqueous 1*M* H_2O_4, 20 mM aniline. Electrode diameter, 1 mm. (b) STM image of the PANI grown in Fig. 3a. V_b = −200 mV, i_t = 1.5 nA. The scanned area is 3 μm × 3 μm. Depth profile along the line is shown at the bottom.

While the scanning area shown in Fig. 3b is 3 by 3 μm, these same features have been observed over 10 by 10 μm areas (the limit of the scan size of the STM head). When the image is carefully examined, fiber bundles of approximately the same volume appear to be oriented at various angles with respect to the substrate. If the lowest position of the STM image is assumed to be the bare Pt surface, a film thickness of ~200-250 Å is found, Fig. 3b. A sample similar to the one in Fig. 3b was used for SEM investigations. The SEM image could not resolve any of the distinct features in Fig. 3b, and showed only a flat structure. In general, SEM images were poor when the surface topography showed thicknesses less than 100 Å. The main advantage of using SEM is the ability to scan an area an order of magnitude larger than STM. That is, if a feature is rare on the surface, SEM provides a higher probability of observing the structure than does STM. However, the resolution of the STM is much greater. Thus, STM and SEM serve as complementary techniques in the investigation of the early growth stages of PANI.

The polymer formed at a 20 V/s scan rate was much denser than that formed at 50 mV/s, even when the amount of charge passed per unit area of electrode was the same. The differences in morphology found by STM, for films prepared at different scan rates were seen at a number of locations on the surface and were found for 2 experiments at each scan rate. These differences can probably be ascribed to kinetic effects. During fast scans, the most rapid reaction [*i.e.*, head-to-tail polymerization (16, 19, 22)] dominates the formation of polyaniline, leading to a film with uniform and well-ordered structures. At slower scan rates, secondary reactions [*e.g.*, tail-to-tail, head-to-head polymerizations, degradation reactions (16, 19, 22)] also occur, leading to a wider distribution of products, less regular polymers, and a rougher, more amorphous film. These results suggest the possibility of electrochemical control of polyaniline morphology. More detailed studies of the effect of concentration and other solution conditions and scan rate on the mechanism of aniline polymerization are in progress (22).

Acknowledgment

The support of this research by grants from the Office of Naval Research and the Texas Advanced Research Program is gratefully acknowledged.

Manuscript submitted June 4, 1991; revised manuscript received September 6, 1991.

The University of Texas assisted in meeting the publication costs of this article.

REFERENCES

1. G. Binnig and H. Rohrer, *Helv. Phys. Acta,* **55,** 726 (1982).
2. G. Binnig, H. Roher, Ch. Gerber, and E. Wiebel, *Phys. Rev. Lett.,* **49,** 57 (1982).
3. G. Binnig and H. Rohrer, *IBM J. Res. Develop.,* **30,** 355 (1986).
4. P. Hansma and J. Tersoff, *J. Appl. Phys.,* **61,** R1 (1987).
5. T. R. Albrecht, H. A. Mizes, J. Nogami, S.-I. Park, and C. F. Quate, *Appl. Phys. Lett.,* **52,** 362 (1989).
6. A. F. Diaz and J. Bargon, in "Handbook of Conducting Polymers," T. A. Skotheim, Editor, pp. 265, Marcel Dekker, New York, NY (1986).
7. D. Bloor, D. A. P. Monkman, G. C. Stevens, K. M. Gheung, and S. Pugh, *Mol. Cryst. Liq. Cryst.,* **187,** 231 (1990).
8. R. Qian and J. Qiu, *Polym. J.,* **19,** 157 (1987).
9. W.-S. Huang, B. D. Humphery, and A. G. MacDiarmid, *J. Chem. Soc. Faraday Trans.,* **82,** 2385 (1986).
10. S. Bruncher and W. Porzio, *Makromol. Chem.,* **89,** 961 (1988).
11. R. Yang, D. F. Evans, L. Christensen, and W. A. Hendrickson, *J. Phys. Chem.,* **94,** 6117 (1990).
12. G. Caple, B. L. Wheeler, R. Swift, T. L. Porter, and S. Jeffers, *ibid.,* **94,** 5639 (1990).
13. I. G. Mantovani, R. J. Warmack, B. K. Annis, A. G. MacDiarmid, and E. J. Scherr, *Appl. Poly. Sci.,* **40,** 1693 (1990).
14. D. Jeon, J. Kim, M. C. Gallagher, R. F. Willis, and Y.-T. Kim, *J. Vac. Sci. Tech.* (in press).
15. D. A. Bonnel and S. Angelopoulo, *Synth. Met.,* **33,** 301 (1989).
16. Y.-B. Shim, M.-S. Won, and S.-M. Park, *This Journal,* **137,** 538 (1990).
17. E. M. Genies and C. Tsintavis, *J. Electroanal. Chem. Interfacial Electrochem.,* **195,** 109 (1985).

18. Deposition was carried out by cycling the potential from −0.6 to 0.7 V *vs.* SMSE using a PAR 173 potentiostat. Under ~1 × 10^{-6} Torr, platinum was sputtered, to a thickness of approximately 2000 Å, on the exposed area (2 mm diameter circular spot) of a glass slide. Aniline (J. T. Baker Inc., Phillipsburg, NJ) was distilled over Zn powder on a vacuum line. After cycling to deposit the film, the potential was stopped at −0.6 V *vs.* SMSE, and the film removed. The resulting PANI (leuco emeraldine form) probably oxidized in air during the STM measurement. The stability of the air oxidized film was tested by spectroscopic ellipsometry; the morphology did not change over at least several hours (20).
19. D. E. Stilwell and S.-M. Park, *This Journal,* **135,** 2491 (1988).
20. Y.-T. Kim, R. W. Collins, D. L. Allara, and K. Vedam, unpublished results. Spectroscopic ellipsometry was used to derive the empirical equation, $T = 12345 \times Q$ (T = thickness (Å), Q = number of coulombs per cm^2 for anodic charging during the potential cycling), to relate the thickness *vs.* total charge consumed during the electropolymerization.
21. Y.-T. Kim, S. A. Hendricks, and A. J. Bard, manuscript in preparation.
22. H. Yang, Ph.D. Thesis, The University of Texas at Austin (in preparation).

Development of "Stainless Aluminum"

F. Mansfeld, V. Wang, and H. Shih

Corrosion and Environmental Effects Laboratory, Department of Materials Science and Engineering, University of Southern California, Los Angeles, California 90089-0241

ABSTRACT

A process for surface modification of Al-based materials is described which involves immersion in boiling $Ce(NO_3)_3$ and $CeCl_3$, followed by anodic polarization in a molybdate solution. Each of these three steps is carried out for 2 h. Al 6061 treated in this manner did not show any signs of uniform or localized corrosion during immersion in 0.5*N* NaCl for 60 days. A sample with a scratch in the modified surface also did not show any corrosion after 25 days in NaCl. Since this surface modification process produces exceptional corrosion resistance, it should be considered as a candidate for the replacement of chromate conversion coatings.

The environmental problems associated with the use of chromate ions in the formation of conversion coatings for Al alloys make it necessary to investigate alternative methods for corrosion protection. Many attempts have been made to increase the corrosion resistance of Al alloys by the formation of surface alloys using ion beam mixing (1) or sputter deposition (2). However, these processes will probably remain restricted to the formation of small areas of modified surfaces. Shaw *et al.* (3) have recently demonstrated an electrochemical process by which Mo-containing species were incorporated into the passive film of thin films on pure Al. The approach taken in this laboratory has previously involved immersion of Al-based materials in rare-earth metal chlorides such as $CeCl_3$, $NdCl_3$, or $PrCl_3$ (4, 5). While very corrosion-resistant surfaces have been obtained in this manner for Al alloys such as Al 6061, and to a lesser degree for Al-based metal matrix composites, the immersion time of one week made this process not very attractive for practical applications.

As will be shown below, the treatment time can be shortened to a few hours by using hot solutions of $Ce(NO_3)_3$ and $CeCl_3$. Exceptional corrosion resistance is obtained, especially when a step involving anodic polarization in a molybdate solution is added (3). Al 6061 treated in this manner did not show any sign of localized corrosion after 60 days immersion in 0.5*N* NaCl (open to air). For an untreated sample or a sample which had been treated only in the molybdate solution, pits initiate within the first day of exposure. A sample which had been scratched did not show uniform or localized corrosion in the scratch after exposure to NaCl for 25 days. These results suggest clearly that the Ce + Mo process described in this paper is a very promising approach in the development of "stainless aluminum" leading eventually to the replacement of chromate conversion coatings.

Methods and Materials

Two different methods of surface preparation have been used. The first involved immersion in hot 10 m*M* $Ce(NO_3)_3$ for 2 h, followed by immersion in hot 5 m*M* $CeCl_3$ for 2 h. In the second method, an electrochemical step was added in which the sample was polarized in deaerated 0.1*M* Na_2MoO_4 at a potential in the passive region (+500 mV *vs.* SCE) for 2 h. The materials were pure Al, Al 6061-T6, Al 2024-T3, and Al/SiC. The properties of the modified surfaces were studied using potentiodynamic polarization tests, electrochemical impedance spectroscopy (EIS), and scanning electron microscopy/energy-dispersive x-ray spectroscopy.

Results and Discussion

Figure 1 shows EIS data for Al 6061 which has been treated in the $Ce(NO_3)_3/CeCl_3/Na_2MoO_4$ process and then immersed in NaCl. The impedance data remained capacitive in the 30-day period shown in Fig. 1, indicating that uniform corrosion was very low and localized corrosion did not occur. As shown elsewhere (6), EIS is very sensitive to the occurrence of localized corrosion on Al-based materials. For untreated Al 6061, the initiation of pits was detected after 1 day of exposure to 0.5*N* NaCl. No changes in the EIS data in Fig. 1 were observed for 60 days, and R_p exceeded 10^7 Ω-cm^2 during the entire test period, corresponding to extremely low corrosion rates. Very similar results were obtained for pure Al; however, less satisfactory behavior occurred for Al 2024 and Al/SiC.

The unique properties of the modified surfaces can be illustrated by the changes in the anodic and cathodic polarization curves obtained in 0.5*N* NaCl (open to air). Starting at E_{corr}, extremely small current densities (in the nA/cm^2 range) were observed for passivated Al 6061 [$Ce(NO_3)_3/CeCl_3/Na_2MoO_4$] in the anodic polarization curve (Fig. 2), until at about −540 mV where the current suddenly increased to about 30 μA/cm^2, followed by an active-to-passive transition and a passive region

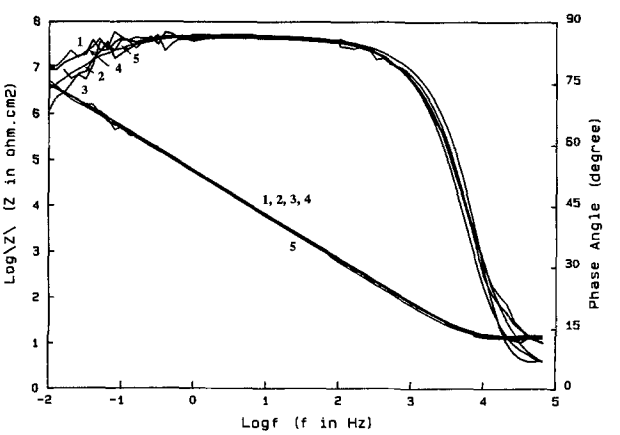

Fig. 1. Bode-plots for Al 6061-T6 (Ce/Mo passivation) as a function of exposure time to 0.5*N* NaCl; curve 1, 6h, curve 2, 1d, curve 3, 7d, curve 4, 14d, curve 5, 30d.